NATIONAL BUREAU OF STANDARDS REPORT

10 388

ELASTIC STABILITY AND DEFLECTIONS OF ECCENTRICALLY-LOADED COMPRESSION MEMBERS MADE OF MATERIAL WITH NO TENSILE STRENGTH

U.S. DEPARTMENT OF COMMERCE
NATIONAL BUREAU OF STANDARDS

NATIONAL BUREAU OF STANDARDS

The National Bureau of Standards [1] was established by an act of Congress March 3, 1901. Today, in addition to serving as the Nation's central measurement laboratory, the Bureau is a principal focal point in the Federal Government for assuring maximum application of the physical and engineering sciences to the advancement of technology in industry and commerce. To this end the Bureau conducts research and provides central national services in four broad program areas. These are: (1) basic measurements and standards, (2) materials measurements and standards, (3) technological measurements and standards, and (4) transfer of technology.

The Bureau comprises the Institute for Basic Standards, the Institute for Materials Research, the Institute for Applied Technology, the Center for Radiation Research, the Center for Computer Sciences and Technology, and the Office for Information Programs.

THE INSTITUTE FOR BASIC STANDARDS provides the central basis within the United States of a complete and consistent system of physical measurement; coordinates that system with measurement systems of other nations; and furnishes essential services leading to accurate and uniform physical measurements throughout the Nation's scientific community, industry, and commerce. The Institute consists of an Office of Measurement Services and the following technical divisions:

Applied Mathematics—Electricity—Metrology—Mechanics—Heat—Atomic and Molecular Physics—Radio Physics [2]—Radio Engineering [2]—Time and Frequency [2]—Astrophysics [2]—Cryogenics.[2]

THE INSTITUTE FOR MATERIALS RESEARCH conducts materials research leading to improved methods of measurement standards, and data on the properties of well-characterized materials needed by industry, commerce, educational institutions, and Government; develops, produces, and distributes standard reference materials; relates the physical and chemical properties of materials to their behavior and their interaction with their environments; and provides advisory and research services to other Government agencies. The Institute consists of an Office of Standard Reference Materials and the following divisions:

Analytical Chemistry—Polymers—Metallurgy—Inorganic Materials—Physical Chemistry.

THE INSTITUTE FOR APPLIED TECHNOLOGY provides technical services to promote the use of available technology and to facilitate technological innovation in industry and Government; cooperates with public and private organizations in the development of technological standards, and test methodologies; and provides advisory and research services for Federal, state, and local government agencies. The Institute consists of the following technical divisions and offices:

Engineering Standards—Weights and Measures — Invention and Innovation — Vehicle Systems Research—Product Evaluation—Building Research—Instrument Shops—Measurement Engineering—Electronic Technology—Technical Analysis.

THE CENTER FOR RADIATION RESEARCH engages in research, measurement, and application of radiation to the solution of Bureau mission problems and the problems of other agencies and institutions. The Center consists of the following divisions:

Reactor Radiation—Linac Radiation—Nuclear Radiation—Applied Radiation.

THE CENTER FOR COMPUTER SCIENCES AND TECHNOLOGY conducts research and provides technical services designed to aid Government agencies in the selection, acquisition, and effective use of automatic data processing equipment; and serves as the principal focus for the development of Federal standards for automatic data processing equipment, techniques, and computer languages. The Center consists of the following offices and divisions:

Information Processing Standards—Computer Information — Computer Services — Systems Development—Information Processing Technology.

THE OFFICE FOR INFORMATION PROGRAMS promotes optimum dissemination and accessibility of scientific information generated within NBS and other agencies of the Federal government; promotes the development of the National Standard Reference Data System and a system of information analysis centers dealing with the broader aspects of the National Measurement System, and provides appropriate services to ensure that the NBS staff has optimum accessibility to the scientific information of the world. The Office consists of the following organizational units:

Office of Standard Reference Data—Clearinghouse for Federal Scientific and Technical Information [3]—Office of Technical Information and Publications—Library—Office of Public Information—Office of International Relations.

---

[1] Headquarters and Laboratories at Gaithersburg, Maryland, unless otherwise noted; mailing address Washington, D.C. 20234.
[2] Located at Boulder, Colorado 80302.
[3] Located at 5285 Port Royal Road, Springfield, Virginia 22151.

NATIONAL BUREAU OF STANDARDS REPORT

NBS PROJECT		NBS REPORT
4212111	November 23, 1970	10 388

ELASTIC STABILITY AND DEFLECTIONS OF ECCENTRICALLY-LOADED COMPRESSION MEMBERS MADE OF MATERIAL WITH NO TENSILE STRENGTH

By

Felix Y. Yokel

U.S. DEPARTMENT OF COMMERCE

NATIONAL BUREAU OF STANDARDS

TABLE OF CONTENTS

Elastic Stability and Deflections of Eccentrically - Loaded Compression Members Made of Material With No Tensile Strength

by

Felix Y. Yokel

A mathematical solution is derived, which permits the computation of critical load, deflection and stresses for eccentrically loaded slender prismatic compression members, made of materials that develop compressive strength but have no tensile strength. A graphical presentation of the solution facilitates its application. In an example of application, the solution is used to compute the strength of masonry walls which were tested by the Structural Clay Products Institute. There is good agreement between computed and measured strength.

Key Words: Buckling, compression members, deflection, equilibrium, load eccentricity, masonry, stability, section cracking, stress distribution, unreinforced concrete.

1. Introduction and Scope

In this paper solutions are derived for the computation of elastic deflections and stability of compression members made of materials with compressive strength and no tensile strength and with a linear relationship between compressive stresses and strains. Computed values could be considered upper limits for deflections and lower limits for critical load of solid prismatic walls made of masonry or unreinforced concrete, since these materials have properties similar to those assumed in the paper. In Appendix III the solutions are used to predict the results of 39 full-scale tests on brick walls which were conducted by the Structural Clay Products Institute[2][1], and the correlation between test results and theory is discussed.

2. Assumed Material Properties and Member Geometry

The material is assumed to be elastic, to have a linear relationship between stress and strain in compression and to have no tensile strength. The problem is analyzed for a prismatic member with a solid rectangular cross section with dimensions as shown in Figure 1.

---

[1] Numbers in brackets refer to literature references listed in Appendix III.

3. Loading Conditions

Loading conditions are shown in Fig. 2. The compressive force P is a lineload which is evenly distributed along the width b of the member. The force is applied at an eccentricity equal to or greater than the kern-eccentricity ($e \geq t/6$). The line of action of force P is parallel to the axis of the undeflected member and the force is applied through hinges at both ends of the member. Thus the ends of the member are not restrained from rotation. The member is also not restrained from shortening in the direction of the compressive force.

4. Equilibrium

4.1 Equilibrium at a Cross Section

Equilibrium at any cross section requires that the resultant reaction force be equal to and collinear with the applied force P. The corresponding stress distribution over a cross section is illustrated in Fig. 3 for two cases.

Figure 3(a) illustrates the case where P acts at an eccentricity equal to kern eccentricity ($e = t/6$). Figure 3(b) illustrates the case where $e > t/6$.

In the case illustrated in Figure 3(a) the compressive stress (σ) at one face (the tension face)[2/] of the cross section is zero. At the other (compression) face, the maximum

---

[2/] The term "tension face" is used here to identify the face that is subjected to zero stress and develops tension cracks, even though no tensile stress can exist in the member.

compressive stress (σ_o) occurs:

$$\sigma_o = \frac{2P}{bt} \quad .$$

In Figure 3(b) a tensile crack appears at the tension side of the cross section, since the material has no tensile strength. The uncracked part of the cross section has a triangular stress distribution similar to that shown in Figure 3(a), where $\sigma = 0$ at the origin of the crack.

The maximum stress at the compression face of the cross section is:

$$\sigma_o = \frac{2P}{3bu} \qquad \text{(eq. 1)}$$

where u is the distance between the action line of force P and the compression face of the cross section.

The uncracked depth of the section in figure 3(b) is 3u, and the depth of the crack is t-3u. The expression in eq. 1 is valid for all cases where $e \geq t/6$. This includes the case in figure 3(a), where $u = t/3$, and:

$$\sigma_o = \frac{2P}{3bu} = \frac{2P}{bt} \quad .$$

4.2 Equilibrium of the Structural Member

The stress distribution within the structural member, when force P is applied at an eccentricity $e \geq t/6$, is illustrated in Fig. 4. The rectangle outlined by broken lines shows the undeflected shape of the member. The deflected shape is shown by the heavy outline. The shaded area within the deflected member shows the uncracked zone which supports the load. The stress distribution at one particular cross section is shown by the heavily -shaded triangle.

The distance between the compression face of the member and the line of action of force P, u, varies along the height of the member, because of member deflection. The maximum distance, u_1, occurs at the two member ends. The minimum distance, u_o, occurs at midheight. The line of action of force P, which is shown in the figure by a dashed line, passes through the edge of the middle third of the compression zone. Since the stress at the compression face of each section, σ_o, is inversely proportional to u, the maximum compressive stress in the member, σ_{max} occurs at midheight:

$$\sigma_{max} = \frac{2P}{3bu_o} \qquad \text{(eq. 2)}$$

5. The Differential Equation for the Deflection Curve

Figure 5 shows the deflection curve of the compression face of the member, together with the coordinate system used. Since the member is symmetrically loaded the origin was assumed at midheight. The x axis is parallel to the action line of P, and is tangential to the deflection curve at the origin. At each point, $u = u_o + y$, and, at $x = h/2$, $u = u_o + y = u_1$.

Figure 6 shows a small element of the deflected member between the compression face and the boundary of the uncracked zone, where $\sigma = 0$ at all times. The element itself is shown by the solid outline. The average depth of the element is 3u. The initial undeflected length is $d\ell$.

The curvature of the compression face is caused by the shortening of the face under compressive stress relative to the boundary of the uncracked zone, which does not change in length since $\sigma = 0$ on the boundary.

As $d\ell \to 0$, the following expression can be written for ϕ, the change in the slope of the deflection curve over the length of the element:

$$\phi = \frac{\varepsilon \, d\ell}{3u}$$

where ε is the average strain over length $d\ell$.

but $$\varepsilon = \frac{\sigma_o}{E} = \frac{2P}{3bu} \cdot \frac{1}{E}$$ (see eq. 1)

where σ_o is the average stress at the compression face over length $d\ell$ and E is Young's modulus of elasticity,

thus $$\phi = \frac{\varepsilon \, d\ell}{3u} = \frac{2P}{9Eb} \cdot \frac{d\ell}{u^2}$$

The length of the compression face of the deflected element, $d\ell\,(1 - \varepsilon)$, can be expressed in terms of the radius of curvature ρ:

$$\rho\phi = d\ell(1 - \varepsilon)$$

or $$\frac{1}{\rho} = \frac{\phi}{d\ell\,(1 - \varepsilon)} = \frac{2P}{9Eb} \, \frac{1}{u^2(1 - \varepsilon)}$$

generally $$\frac{1}{\rho} = \frac{d^2y/dx^2}{[1 + (dy/dx)^2]^{3/2}}$$

The following equation can therefore be written for d^2y/dx^2:

$$\frac{d^2y}{dx^2} = \frac{2P}{9Eb} \, \frac{[1 + (dy/dx)^2]^{3/2}}{u^2(1 - \varepsilon)}$$

This derivation is envisioned to apply to materials which develop relatively small strain ($\varepsilon < 0.005$). The quantity $1 - \varepsilon$ will therefore approximately equal unity. The maximum deflection developed will also be small relative to the height of the member, and the slope of the deflection curve dy/dx, will be much smaller than 1 even at the point of maximum slope. The following approximation will therefore cause errors which are of lower-order magnitude and do not appreciably affect the result:

$$\frac{[1 - (dy/dx)^2]^{3/2}}{1 - \varepsilon} \simeq 1$$

A similar assumption is traditionally made in derivations of elastic deflections and critical loads for conventional structural members.

thus the expression for d^2y/dx^2 reduces to:

$$\frac{d^2y}{dx^2} = \frac{1}{\rho} = \frac{2P}{9Eb} \cdot \frac{1}{u^2}$$

Since the value $\frac{2P}{9Eb}$ is constant for any particular member, the constant:

$K_1 = \frac{2P}{9Eb}$ is substituted into the equation.

furthermore: $u = u_o + y$.

The following differential equation can therefore be written:

$$\frac{d^2y}{dx^2} = \frac{K_1}{(u_o+y)^2} \qquad \text{(eq. 3)}$$

where: $K_1 = \frac{2P}{9Eb}$ = constant .

The following three boundary conditions apply to this equation (refer to Fig. 5):

at $x = 0$, $y = 0$ (1)

at $x = 0$, $\frac{dy}{dx} = 0$ (2)

at $x = h/2$; $y = u_1 - u_o$ (3)

6. Solution to the Differential Equation for the Deflection Curve

An exact solution for eq. 3 has been derived. Detailed steps of that derivation are presented in Appendix II. The following equation has been derived for the deflection curve:

$$x = \pm \frac{3}{2} \sqrt{\frac{Ebu_o}{P}} \left[\sqrt{y\,(u_o + y)} + u_o \ln\left(\frac{\sqrt{y} + \sqrt{u_o + y}}{\sqrt{u_o}} \right) \right] \qquad \text{(eq. 4)}$$

if boundary condition (3): at $h/2$; $y = u_1 - u_o$ is substituted into this equation, the following relationship between P, u_1, and u_o can be derived (See Appendix II):

$$\frac{P}{P_{ec}} = 0.40528\,\alpha\left[\sqrt{1-\alpha} + \alpha\, ln\left(\sqrt{\frac{1-\alpha}{\alpha}} + \sqrt{\frac{1}{\alpha}}\right)\right]^2$$

where:

$$P_{ec} = \frac{\pi^2 E I_e}{h^2}$$

The term P_{ec} is an "equivalent" critical load, computed from an "equivalent" I, which is based on an "equivalent" thickness of $3u_1$.

$$I_e = \frac{27 b u_1^3}{12}$$

therefore $$P_{ec} = \frac{27}{12} \cdot \frac{\pi^2 E b u_1^3}{h^2}$$

P_{ec} becomes the Euler load P_c when the section is loaded at the edge of the kern ($3u_1 = t$).

$\alpha = \frac{u_o}{u_1}$ is a measure of the magnitude of the maximum deflection.

7. Application of the Solution to Derive Critical Load, Maximum Deflection and Maximum Stress

Figure 7 shows a graphical presentation of equation 5. The plot is non dimensional and can be used to solve any particular numerical problem.

Values of P/P_{ec} are plotted along the ordinate. On the abscissa, values of u_o/u_1 are plotted. It can be seen that each value of P/P_{ec} corresponds to two values of u_o/u_1, except for the highest value of P/P_{ec} that can be maintained by the member. The plot of the solution is interpreted as follows:

The value $u_o/u_1 = 1$ corresponds to an undeflected section. Thus this corresponds to no axial load or $P/P_{ec} = 0$. Obviously, no axial load could be maintained if u_o vanishes or $u_o/u_1 = 0$, since the mid section would be cracked over the full width, t. Thus the value $P/P_{ec} = 0$ also corresponds to $u_o/u_1 = 0$.

When P is applied to an undeflected member and increased, deflections would increase correspondingly and the value of u_o/u_1 would decrease. This corresponds to the portion of the curve between $u_o/u_1 = 1$ and $u_o/u_1 = 0.625$, which represents a condition of stable equilibrium. At the value of $u_o/u_1 = 0.625$ the maximum load is applied that the member can support, provided compressive strength was not exceeded at a lower value of P/P_{ec}. Any further increase of P beyond this point would cause the member to collapse.

Thus the important conclusion is reached, that elastic instability will occur at the critical load of:

$$P_{cr} = 0.285\ P_{ec}$$

where $P_{ec} = \dfrac{27\pi^2\ Ebu_1^3}{12\ h^2}$

or $P_{cr} = 0.64\ \dfrac{\pi^2\ Ebu_1^3}{h^2}$ (eq. 6)

The values of P/P_{ec} corresponding to values of u_o/u_1 in the range: $0.625 > u_o/u_1 > 0$ have little physical significance. They correspond to a second deflection that can be maintained by loads smaller than the critical load in a state of unstable equilibrium.

Maximum stresses in the member, corresponding to any load smaller than the critical load (P_{cr}), can also be computed using the plot in Fig. 7 to compute u_o, and eq. 2 to compute maximum stress:

$$\sigma_{max} = \frac{2P}{3bu_o}$$

8. Summary of Theoretical Analysis

For the prismatic member shown in Fig. 1, made of material with no tensile strength, and subjected to the loading condition shown in Fig. 2. The following values can be computed from an exact solution to the differential equation for the deflection curve:

* The critical load:

$$P_{cr} = 0.64 \frac{\pi^2 E b u_1^3}{h^2} \qquad \text{(eq. 6)}$$

* The maximum compressive stress:

$$\sigma_{max} = \frac{2P}{3bu_o} \qquad \text{(eq. 2)}$$

where u_o can be determined from Fig. 7.

* The maximum deflection can be derived from Fig. 7.

9. Application of the Theory to Predict the Results of Full-Scale Tests on Masonry Walls

9.1 Source of Test Results and Test Specimens

Only few test data are available which fit the boundary conditions and material properties assumed in this paper. The test results chosen for comparison were published by the Structural Clay Products Institute (SCPI) [2], and represent 39 tests on full-scale brick walls of various slenderness ratios (h/t), loaded as shown in Fig. 2. Loads were applied at two eccentricities: $e = t/6$, and $e = t/3$. The walls were solid walls of single- and double-wythe construction, built in running bond. Slenderness ratios varied from $h/t = 6.6$ to $h/t = 46.1$. Mortar was ASTM type S [1] and the compressive strength of the masonry (f'_m) varied from 4,160 psi to 5,100 psi.

9.2 Comparison of the Assumed Material Properties with the Properties of the Test Specimens.

While brick masonry has material properties similar to those assumed in the solution presented in this paper, several differences between the properties of the test specimens and the assumed idealized properties should be noted:

(1) The masonry used in the specimens tested should be expected to develop tensile strength of an order of magnitude of 2-3 percent of its compressive strength. This property would somewhat change the equilibrium conditions illustrated in Fig. 3, which were assumed in the derivation. The change should result in somewhat greater-than-predicted capacities. The discrepancy would be greatest where stability failure occurs at relatively low stress levels (large slenderness ratios and eccentricities).

(2) The stress-strain curve for brick is not exactly linear. The tangent modulus of elasticity at failure tends to be about 70 percent of the initial, tangent modulus of elasticity [3]. If deflections are predicted on the basis of the modulus of elasticity at low stress levels, deflections at high stress levels would probably be greater than the predicted deflections. This change in stiffness also slightly modifies the stress distribution shown in Fig. 3. These effects will increase with increasing stress levels at failure. (Small slenderness ratios and eccentricity).

(3) The brick units themselves have greater strength and stiffness than the mortar beds connecting the units. This discontinuity results in a stress distribution which is much more complex than the idealized stress

distribution assumed in the solution. The net effect of these discontinuities on strength and stiffness has not been evaluated.

9.3 Equations for Strength Calculations

The test results presented by SCPI were obtained from a variety of brick walls, and for the sake of comparison, individual tests were normalized by dividing the vertical load carried by each wall by P_o, the load capacity of a cross section subjected to axial compression: $P_o = f'_m bt$. The value of f'_m, the compressive strength under axial load, was in each case derived from the average strength of short brick prisms which were constructed from similar brick and mortar at the time the corresponding test specimens were constructed and which were cured under similar conditions. It has been observed for brick masonry [3] that compressive strength in flexure exceeds the compressive strength in axial compression and that the strength increases with increasing strain gradients. In this case it has been determined that cross sectional capacity of walls loaded at t/6 and t/3 eccentricities can be approximately computed by using the stress distribution in Fig. 3 and assuming a compressive strength in flexure equal to 1.6 times the strength in axial compression: $af'_m = 1.6f'_m$.

It was also determined, that for the walls tested, the modulus of elasticity is predicted with sufficient accuracy by assuming the fixed ratio of: $f'_m/E = 1.215 \times 10^{-3}$.

The following equations can therefore be derived:

Cross Sectional Capacity:

at $e = t/6$: $P_u = 0.8\ P_o$

at $e = t/3$: $P_u = 0.4\ P_o$

Wall Capacity:

Walls may either fail when the flexural compressive strength is exceeded or when elastic instability occurs. For the case of a compression failure, wall capacity may be computed from eq. 2:

at $e = t/6$: $P_u = 0.8\ P_o \frac{u_o}{u_1}$

and $\frac{P_u}{P_o} = 0.8 \frac{u_o}{u_1}$

at $e = t/3$: $P_u = 0.4\ P_o \frac{u_o}{u_1}$

and $\frac{P_u}{P_o} = 0.4 \frac{u_o}{u_1}$

where $\frac{u_o}{u_1}$ can be determined from Fig. 7.

For a stability failure the following equations can be derived from eq. 6:

$$P_{cr} = 0.64 \frac{\pi^2 E b u_1^3}{h^2} = 0.64 \frac{\pi^2 E b t^3}{27\ h^2} \cdot \left(\frac{3u_1}{t}\right)^3$$

$$E = (f'_m/1.215) \cdot 10^3$$

and $P_o = f'_m\, bt$

$$P_{cr} = 192\, P_o \left(\frac{t}{h}\right)^2 \left(\frac{3u_1}{t}\right)^3$$

$$\frac{P_{cr}}{P_o} = \frac{192}{(h/t)^2} \left(\frac{3u_1}{t}\right)^3$$

for $e = t/6$; $\quad 3u_1 = t$

and $$\frac{P_{cr}}{P_o} = \frac{192}{(h/t)^2}$$

for $e = t/3$; $\quad 3u_1 = \frac{t}{2}$

and $$\frac{P_{cr}}{P_o} = \frac{24}{(h/t)^2}$$

The following general equations for wall capacity as a fraction of P_o therefore apply:

at $e = t/6$:

$$\frac{P_u}{P_o} = 0.8\, \frac{u_o}{u_1}$$

or $$\frac{P_u}{P_o} = \frac{192}{(h/t)^2}$$

whichever is smaller (eq. 7)

at $e = t/3$:

$$\frac{P_u}{P_o} = 0.4\, \frac{u_o}{u_1}$$

or $$\frac{P_u}{P_o} = \frac{24}{(h/t)^2}$$

whichever is smaller (eq. 8)

9.4 Comparison of Theory with Test Results

Curves based on equations 7 and 8 are plotted in Fig. 8. Note that for the t/6 eccentricity compression failure occurs at slenderness ratios smaller than 22 ($h/t < 22$). For the t/3 eccentricity compression failure occurs at slenderness ratios smaller than 11 ($h/t < 11$).

In Fig. 9 the theoretical curves are compared with test results. Test results at t/6 eccentricity are shown by the triangles and should be compared with the corresponding curve. Test results at the t/3 eccentricity are shown by the circles.

In general the trend of the test results is correctly predicted by theory and the magnitude of the load capacity is approximately predicted. For the t/6 eccentricity capacity was overestimated for $h/t = 14$ by about 10%. At $h/t = 46$ the capacity was underestimated by a substantial margin, probably because at this low stress level, the effect of the tensile strength is significant. For all other slenderness ratio the average capacity was approximately predicted. For the t/3 eccentricity the capacity also tended to be underestimated at very low failure-stress levels, however, in the range of stability failure, the theoretical curve tends to approach the lower limit of the measured capacities.

9.5 Conclusion From the Comparison of the Theory with Test Results

The theory correctly predicted the trend of the test results and approximately predicted the magnitude of measured capacities. Since equations 7 and 8 are simple and relatively easy to use, their practical application should be seriously considered.

Appendix I. - Notation

af'_m flexural compressive strength of masonry

b width of member

e load eccentricity

$d\ell$ incremental length

E Young's modulus of elasticity

f'_m compressive strength of masonry under axial load

h height of member

K_1 constant $(\frac{2P}{9Eb})$

I moment of inertia $(\frac{bt^3}{12})$

I_e equivalent moment of inertia $(\frac{27bu^3}{12})$

P compressive force applied to member

P_c critical (Euler) load $(\frac{\pi^2 EI}{h^2})$

P_{ec} "equivalent" critical load $(\frac{\pi^2 EI_e}{h^2})$

P_{cr} critical load of member

P_o cross sectional axial-load capacity

P_u load capacity under eccentric vertical compressive load

t thickness of member

u distance between line of action of compressive load and compression face of member

u_o distance between line of action of compressive load and compression face of member at midheight

u_1 distance between line of action of compressive load and compression face of member at member support

α dimensionless parameter $\frac{u_o}{u_1}$

ε strain

ϕ change in slope of deflection curve

ρ radius of curvature

σ compressive stress

σ_o maximum compressive stress in cross section

σ_{max} maximum compressive stress in member

APPENDIX II

DERIVATION OF SOLUTION

$$\frac{d^2y}{dx^2} = \frac{K_1}{(u_o + y)^2}, \text{ where } K_1 = \frac{2P}{9bE}$$

Boundary Conditions:

at $x = 0$, $y = 0$

at $x = 0$, $\frac{dy}{dx} = 0$

at $x = \frac{h}{2}$, $y = u_1 - u_o$

$$\frac{2dy}{dx}\frac{d^2y}{dx^2} = \frac{2K_1}{(u_o + y)^2}\frac{dy}{dx} = \frac{d}{dx}\left(\frac{dy}{dx}\right)^2$$

$$\left(\frac{dy}{dx}\right)^2 = 2K_1\int\frac{dy}{(u_o + y)^2} = -2K_1\frac{1}{u_o + y} + C_1$$

at $y = 0$, $\frac{dy}{dx} = 0$;

$$\therefore C_1 = \frac{2K_1}{u_o}$$

$$\left(\frac{dy}{dx}\right)^2 = 2K_1\left(\frac{1}{u_o} - \frac{1}{u_o + y}\right) = \frac{2K_1}{u_o}\frac{y}{u_o + y}$$

$$\frac{dy}{dx} = \pm\sqrt{\frac{2K_1}{u_o}}\left(\frac{y}{u_o + y}\right)^{1/2}$$

Assume $K_2 = \sqrt{\frac{2K_1}{u_o}} = \frac{2}{3}\sqrt{\frac{P}{Ebu_o}}$

then: $\frac{dy}{dx} = \pm K_2\left(\frac{y}{u_o + y}\right)^{1/2}$

or $dx = \pm\frac{1}{K_2}\left(\frac{u_o + y}{y}\right)^{1/2} dy$

$$x = \pm \frac{1}{K_2} \int \left(\frac{u_o + y}{y} \right)^{1/2} dy$$

$$\int \left(\frac{u_o + y}{y} \right)^{1/2} dy = \sqrt{y\,(u_o + y)} + \frac{u_o}{2} \int \frac{dy}{\sqrt{y\,(u_o + y)}}$$

$$= \sqrt{y\,(u_o + y)} + u_o \, ln\,(\sqrt{y} + \sqrt{u_o + y})$$

$$\therefore \quad x = \pm \frac{1}{K_2} \left[\sqrt{y\,(u_o + y)} + u_o \, ln\,(\sqrt{y} + \sqrt{u_o + y}) \right] + C_2$$

at $x = 0$, $y = 0$;

$$0 = \frac{1}{K_2} \left[0 + u_o \, ln \sqrt{u_o} \right] + C_2 = \frac{1}{K_2} u_o \, ln \sqrt{u_o} + C_2$$

$$\therefore \quad C_2 = - \frac{u_o}{K_2} ln \sqrt{u_o}$$

$$x = \pm \frac{1}{K_2} \left[\sqrt{y\,(u_o + y)} + u_o \, ln \left(\frac{\sqrt{y} + \sqrt{u_o + y}}{\sqrt{u_o}} \right) \right]$$

Substituting K_2

$$x = \pm \frac{3}{2} \sqrt{\frac{Ebu_o}{P}} \left[\sqrt{y\,(u_o + y)} + u_o \, ln \left(\frac{\sqrt{y} + \sqrt{u_o + y}}{\sqrt{u_o}} \right) \right]$$

Solving for u_o:

at $x = \frac{h}{2}$, $y = u_1 - u_o$;

$$\frac{h}{2} = \pm \frac{3}{2} \sqrt{\frac{Ebu_o}{P}} \left[\sqrt{u_1\,(u_1 - u_o)} + u_o \, ln \left(\sqrt{\frac{u_1 - u_o}{u_o}} + \sqrt{\frac{u_1}{u_o}} \right) \right]$$

$$\text{or} \quad P = \frac{9Ebu_o}{h^2} \left[\sqrt{u_1\,(u_1 - u_o)} + u_o \, ln \left(\sqrt{\frac{u_1 - u_o}{u_o}} + \sqrt{\frac{u_1}{u_o}} \right) \right]^2$$

Assume $\alpha = \frac{u_o}{u_1}$

$$P = \frac{9Eu_1^{\,3}}{h^2} \alpha \left[\sqrt{1 - \alpha} + \alpha ln \left(\sqrt{\frac{1 - \alpha}{\alpha}} + \sqrt{\frac{1}{\alpha}} \right) \right]^2$$

Let $P_{ec} = \frac{27\pi^2 Eu^3}{12h^2}$ = "equivalent" critical load

then: $\frac{P}{P_{ec}} = 0.40528\,\alpha\left[\sqrt{1-\alpha} + \alpha\, ln\left(\sqrt{\frac{1-\alpha}{\alpha}} + \sqrt{\frac{1}{\alpha}}\right)\right]^2$

or $\frac{P}{P_{ec}} = f(\alpha)$

Appendix III - References

[1] American Society for Testing Material, "ASTM C270-68, Standard Specifications for Mortar for Unit Masonry", Philadelphia, Pa., 1968

[2] Structural Clay Products Institute, Recommended Practice for Engineered Brick Masonry, Tables 5-20 and 5-21, McLean, Va., November 1969

[3] Yokel, F. Y., Mathey, R. G. and Dikkers, R. D., "Strength of Masonry Walls Under Compressive and Transverse Load", Building Science Series 34, National Bureau of Standards, Washington, D.C., January 1971

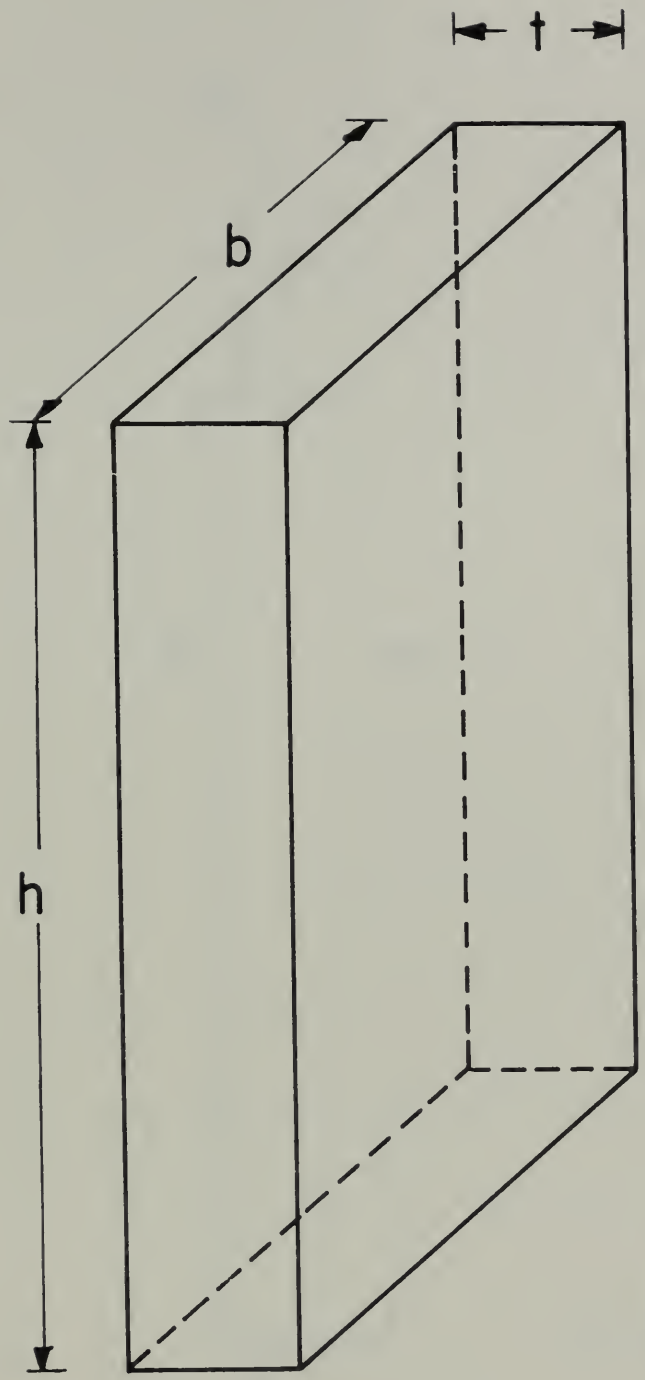

Figure 1. Geometry and Dimensions of Member

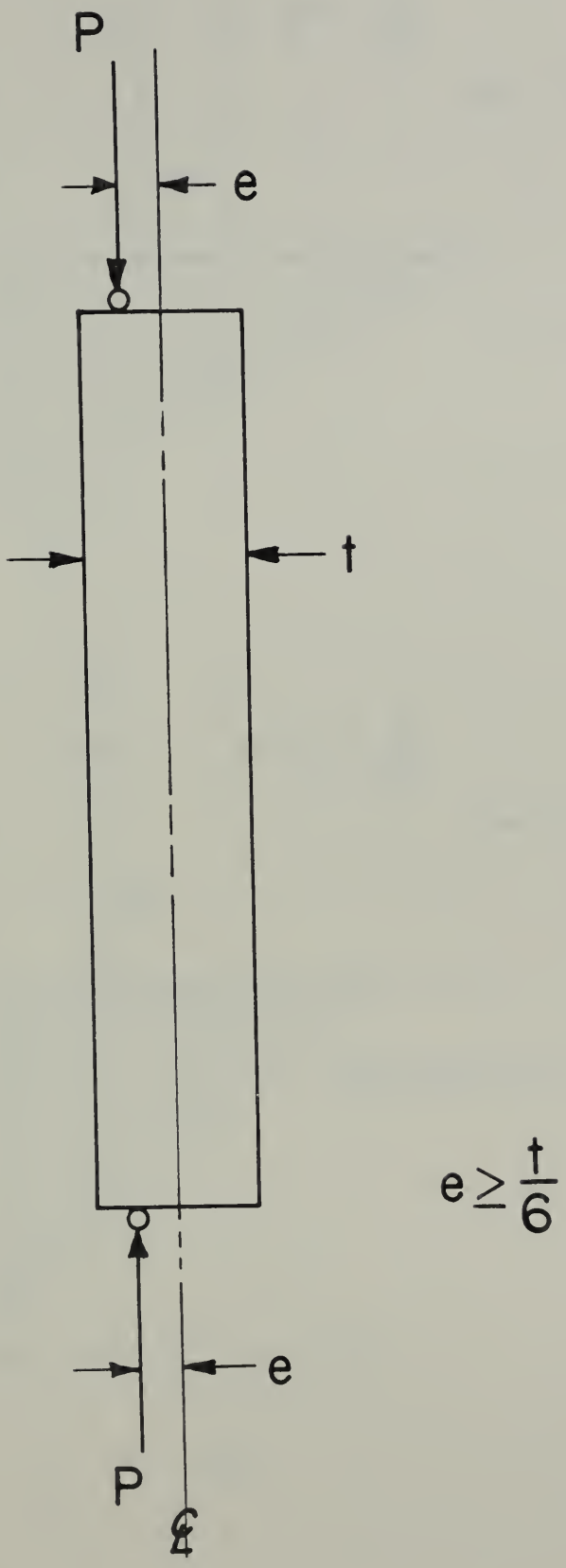

Figure 2. Loading Conditions

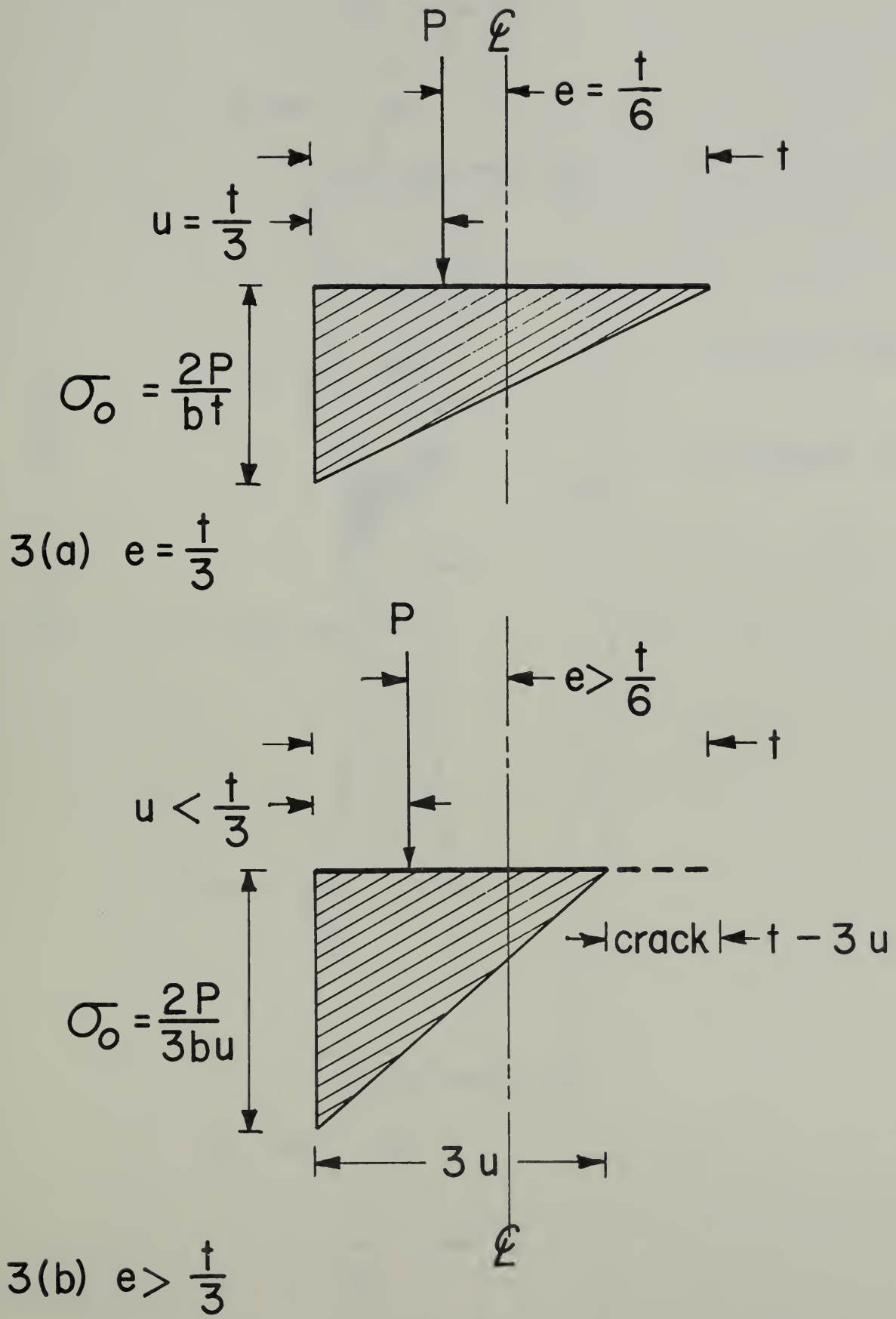

Figure 3. Equilibrium at a Cross Section

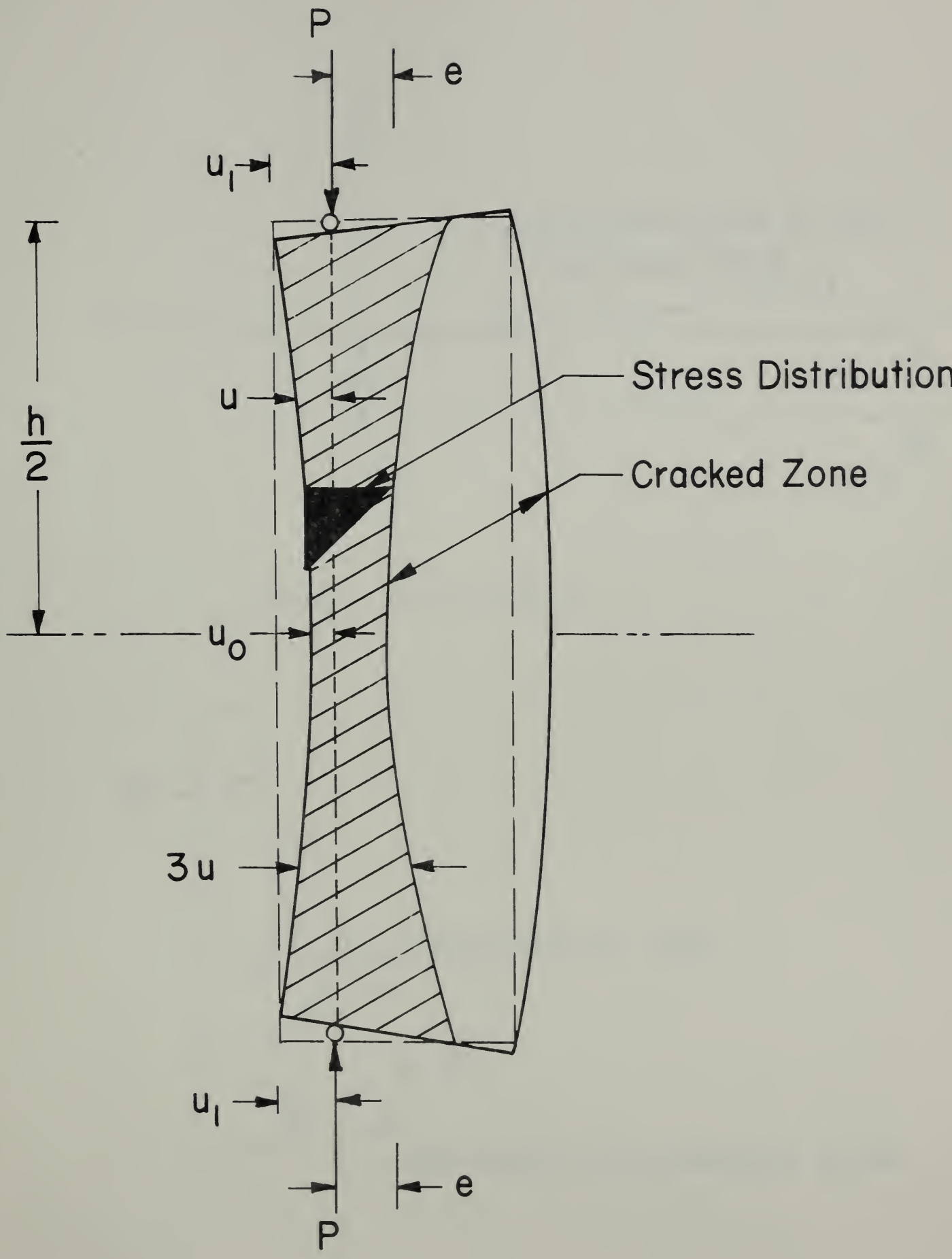

Figure 4. Equilibrium of Member

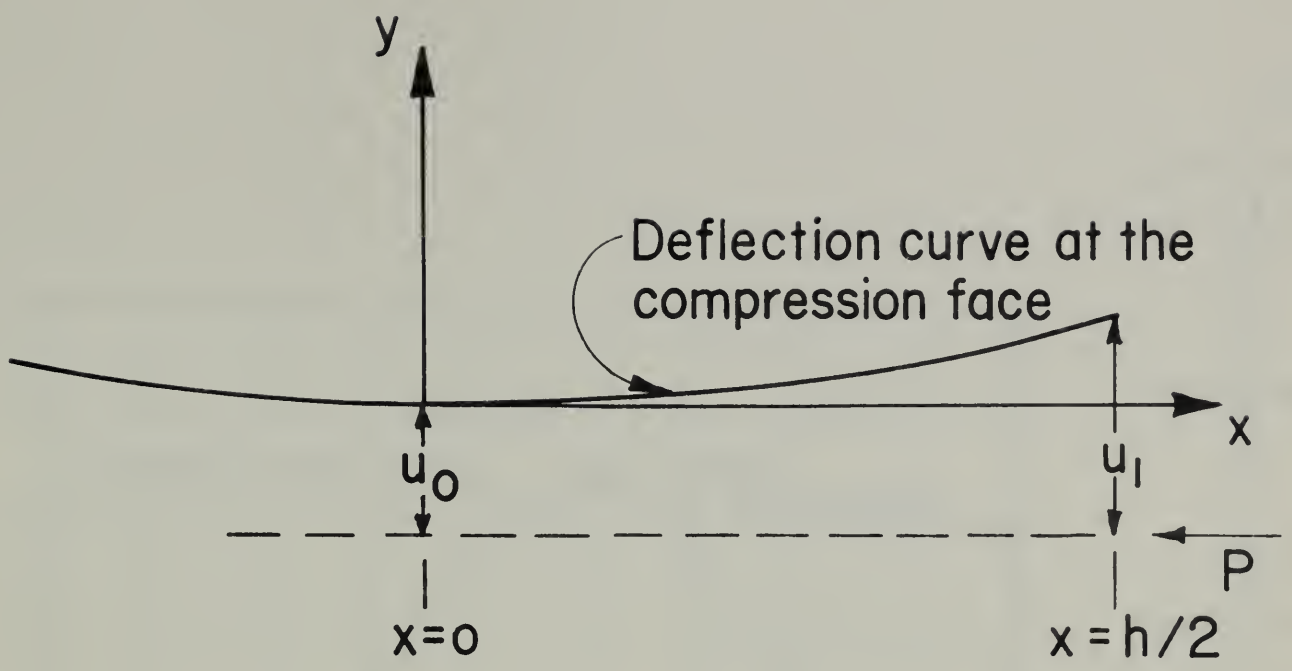

Figure 5. Deflection Curve

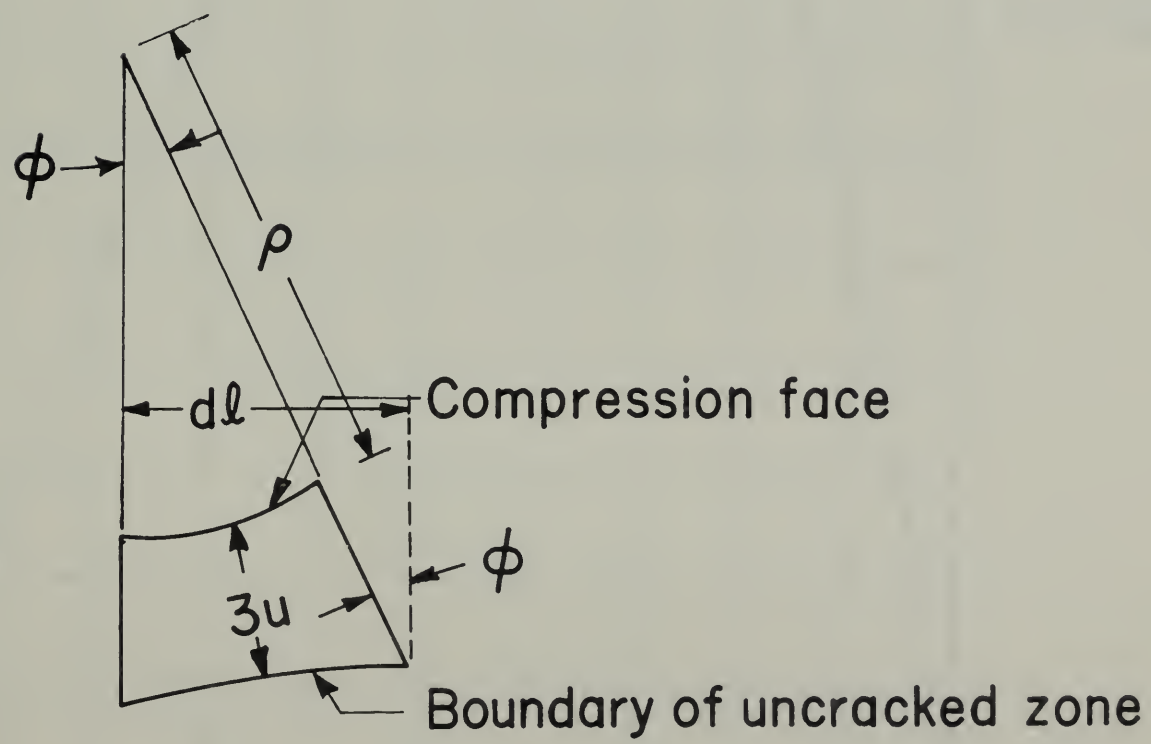

Figure 6. Curvature

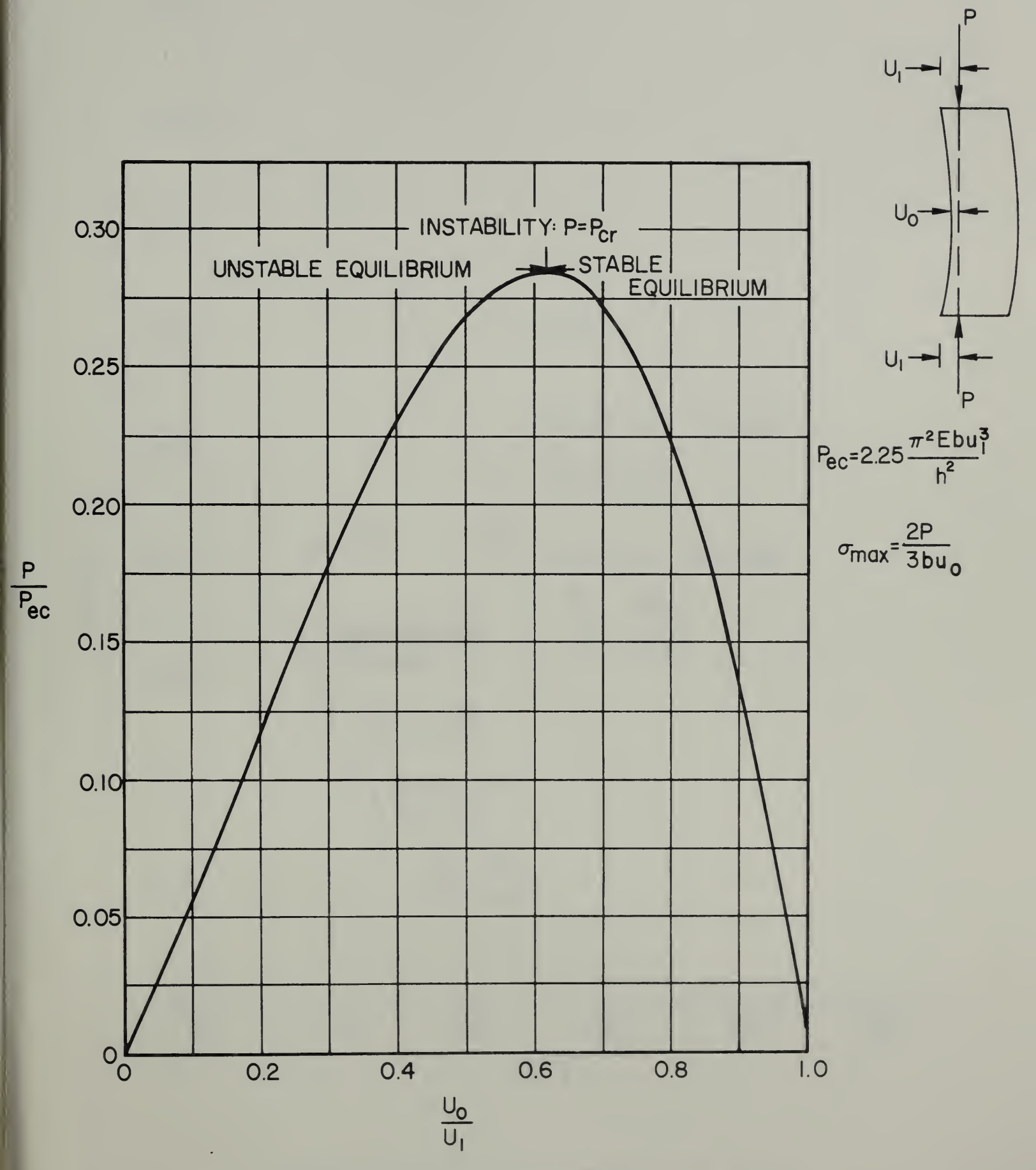

Figure 7. Graphical Presentation of Solution

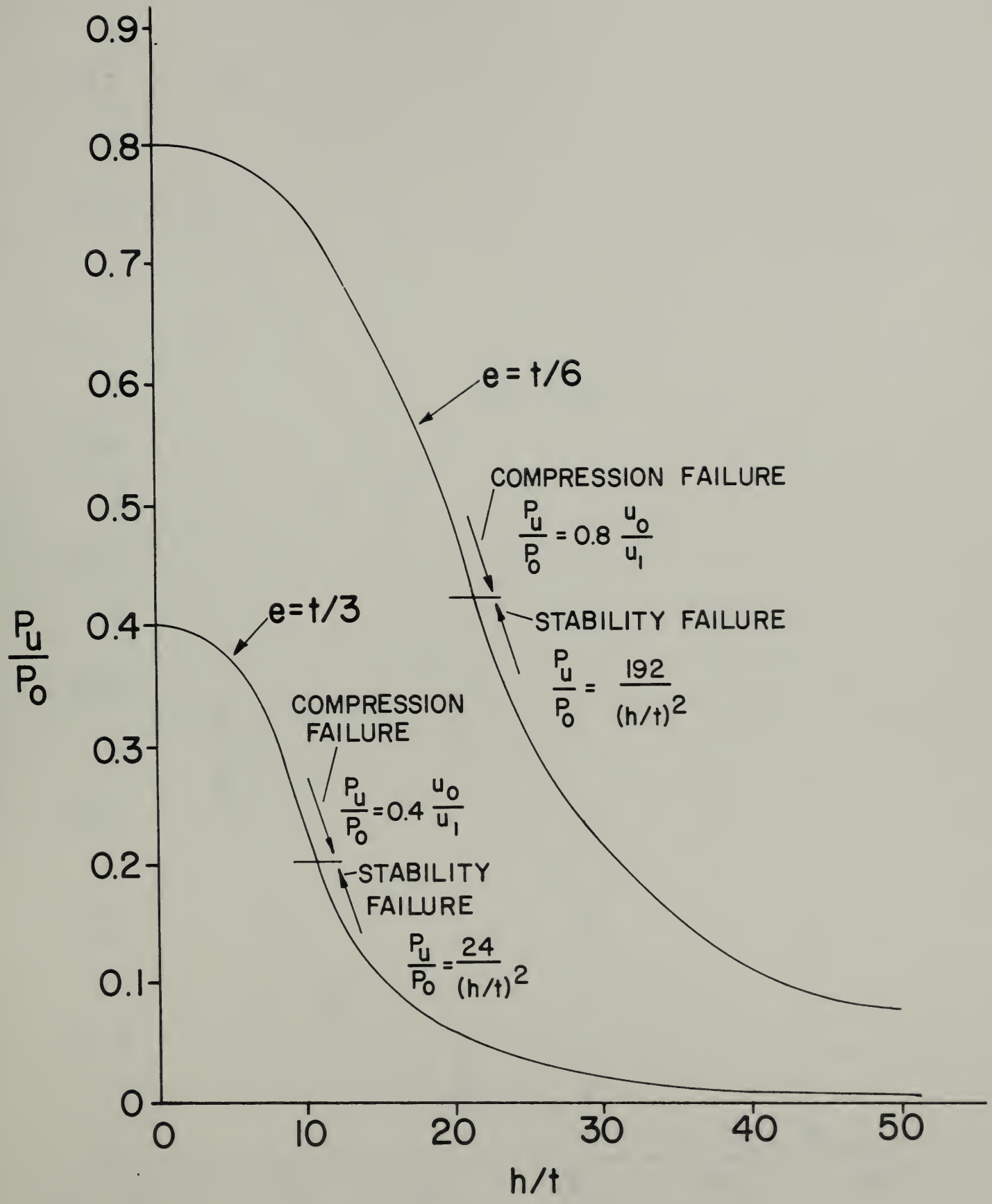

Figure 8. Theoretical Strength of the Tested Walls as a Function of the Slenderness Ratio

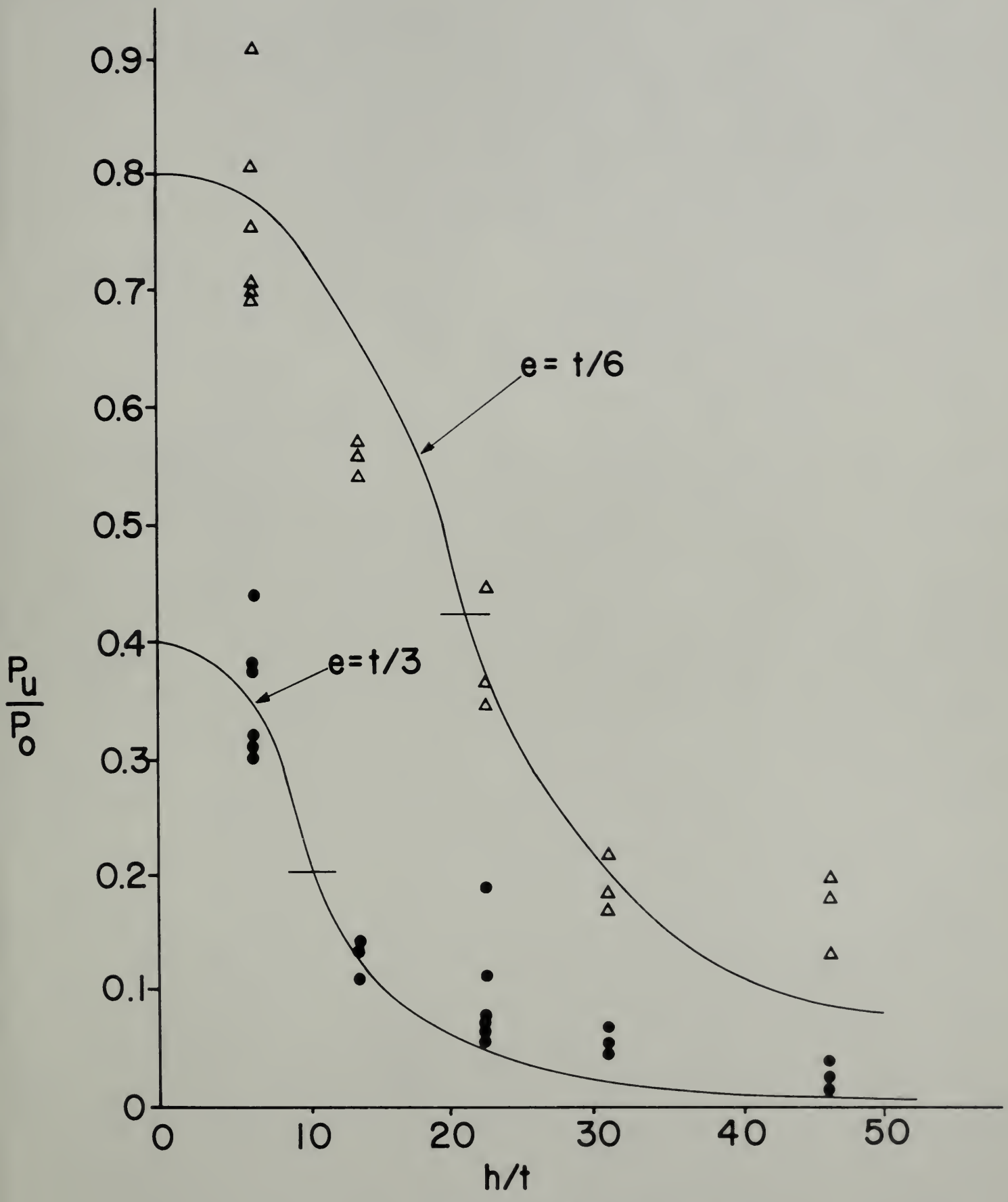

Figure 9. Comparison of the Theory with Test Results


DEPARTMENT OF COMMERCE
NATIONAL BUREAU OF STANDARDS